

Giant dielectric permittivity and magnetocapacitance in $\text{La}_{0.875}\text{Sr}_{0.125}\text{MnO}_3$ single crystalsR. F. Mamin,^{1,2,*} T. Egami,^{1,3,4} Z. Marton,^{3,5} and S. A. Migachev²¹*Department of Physics and Astronomy, University of Tennessee, Knoxville, Tennessee 37996, USA*²*Zavoisky Physical-Technical Institute of RAS, Kazan 420029, Russia*³*Department of Materials Science and Engineering, University of Tennessee, Knoxville, Tennessee 37996, USA*⁴*Oak Ridge National Laboratory, Oak Ridge, Tennessee 37831, USA*⁵*Department of Materials Science and Engineering, University of Pennsylvania, Philadelphia, Pennsylvania 19104, USA*

(Received 6 December 2006; published 29 March 2007)

We report the observation of extremely high dielectric permittivity exceeding 10^9 and magnetocapacitance of the order of $10^4\%$ in $\text{La}_{0.875}\text{Sr}_{0.125}\text{MnO}_3$ single crystal. This phenomenon is observed below 270 K, and it exhibits a history dependence. These effects may be the consequence of strong competition and interplay among the charge, orbital, and spin degrees of freedom, resulting in nanoscale charge and spin dynamic inhomogeneities in the prepercolation regime of the phase segregation.

DOI: [10.1103/PhysRevB.75.115129](https://doi.org/10.1103/PhysRevB.75.115129)

PACS number(s): 77.22.-d, 71.45.-d, 75.47.Lx

The complex interplay and competition among charge, spin, orbital, and lattice degrees of freedom are believed to be the origin of the unexpected magnetic and transport phenomena observed in manganites, such as the colossal magnetoresistance (CMR).¹⁻³ The perovskite manganites $\text{La}_{1-x}\text{Sr}_x\text{MnO}_3$ (LSM- x) have been extensively investigated in the past decade, and LSM- x crystals became the model object for the investigations of colossal magnetoresistance.⁴⁻¹⁰ The recent observation¹¹ of large magnetoelectric and magnetocapacitive effects in pure manganites with the composition RMnO_3 (where R =rare-earth ion) rekindled new interest in these materials. While the search for materials with magnetocapacitive effects has mainly focused on insulating multiferroic materials,^{11,12} it should be possible to attain such effects through manipulation of intrinsic inhomogeneity which is widely observed in doped manganites.¹³ For this purpose we carried out investigations of dielectric properties and the magnetocapacitance effect in a single crystal of doped manganite $\text{La}_{0.875}\text{Sr}_{0.125}\text{MnO}_3$ (LSM-0.125), which we present in this paper.

The LSM-0.125 composition is known to have a complex phase behavior and undergo several transitions upon cooling.⁶⁻¹⁰ At temperature $T_{RO} \approx 450$ K, structural transition from rhombohedral to weakly distorted orthorhombic (O) phase occurs. At temperature $T_{JT} \approx 270$ K, structural transition from a weakly distorted orthorhombic phase to a strongly distorted Jahn-Teller orthorhombic (O') phase takes place. Magnetism sets in at $T_{CA} \approx 180$ K, but the exact nature of the magnetic order is unclear⁵⁻¹⁰ and will be addressed in this paper. Below $T_p \approx 140$ K the system becomes an insulating ferromagnet with orbital ordering in the orthorhombic (O'') phase.^{6,10} The details of this phase behavior are controversial and updated continuously.^{3,6,10} Moreover, the LSM- x material presents a very complex phase diagram, especially at a low Sr doping.³ Furthermore, the experimental evidence for inhomogeneous states in manganites is simply overwhelming.^{3,9,14-16} These inhomogeneities appear even above the Curie temperature, and the new scale of temperature, T^* should be introduced.³ Below T^* the metallic clusters start forming and their percolation may lead to long-range

order as well as CMR effect. In our experiments, an attempt for characterizing T^* was made in the regime where percolation is not complete.

The low-frequency dielectric properties of doped manganites have been studied previously.¹⁷⁻¹⁹ In some works, two-point probe method was used for dielectric measurements,^{17,18} resulting in effects produced by the contact areas.²⁰ In polycrystalline films they found the effect of a barrier-layer capacitor microstructure created during deposition and oxidation of grain-boundary regions, which form an insulating shell on semiconducting grains.¹⁹ In order to determine the intrinsic dielectric properties of the manganites in this work, we studied the effect of magnetic field on the low-frequency dielectric response using the four-point probe method. We show that the low-frequency dielectric and magnetic measurements are indicative of charge separation in LSM-0.125. We also find that the dielectric permittivity displays a nonergodic behavior and is strongly dependent on how the magnetic field is applied and that giant dielectric permittivity up to 10^9 and magnetocapacitance up to $10^4\%$ are observed.

The dielectric measurements were carried out on a high-quality right-angled-parallelepiped LSM-0.125 single crystal with the sizes of $5.13 \times 5.13 \times 7.50$ mm³ and with the c axis parallel to the long axis. The magnetic measurements were done on a cylindrical single crystal with diameter 2.47 mm and with length 1.77 mm. These crystals were characterized in earlier works.^{6,10} The complex dielectric permittivity was measured by the four-point probe method on a precision impedance analyzer Agilent 4294A and a Quantum Design physic properties measurement system 6100 (PPMS 6100) in the temperatures range of 80–350 K and at frequencies ranging from 10 Hz to 10 MHz in the weak probe electric field applied along the polar c axis. Two electrodes were attached to the square surfaces to apply the ac voltage, and two small electrodes were attached on one of the ac-dc surfaces. The distance between small electrodes was 2.5–3.5 mm. The magnetic measurements were made on a Quantum Design magnetic properties measurement system (MPMS) in the temperatures range of 80–350 K.

The temperature dependence of the dielectric permittivity, $\epsilon(T)$, on cooling at zero external magnetic field [zero-field

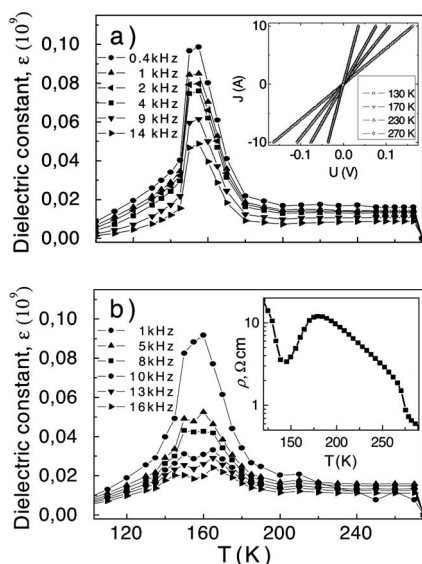


FIG. 1. Temperature dependence of the dielectric permittivity $\varepsilon(T)$ at different frequencies f at zero external magnetic field: (a) ZFC and (b) ZFHaFC regimes; the insets show the I - V characteristics at 130, 170, 230, and 270 K and the temperature dependence of the dc resistivity, $\rho(T)$.

cooled (ZFC)] is shown in Fig. 1(a) and the same quantity at zero external magnetic field after field cooling in 2 T (ZFHaFC) is shown in Fig. 1(b). The value of $\varepsilon(T)$ is obtained from the measured capacitance. The inset in Fig. 1(a) shows the I - V characteristics at several temperatures, indicating good Ohmic behavior. The temperature dependence of the dc resistivity $\rho(T)$ is shown in the inset of Fig. 1(b). The ac resistivity of the sample in the low-frequency range coincides with its dc resistivity and increases slowly at high frequencies. It is found that for the case of ZFC the value of $\varepsilon(T)$ increases up to 10^7 below $T \sim 270$ K and does not vary much in the temperature range of 180–270 K, but it rapidly increases below $T \sim 180$ K, forming a sharp peak at temperature ~ 150 K. It is noted that the maximum of the $\varepsilon(T)$ value corresponds to the minimum in the resistivity [see the inset in Fig. 1(b)]. The sharp decrease of the dielectric permittivity at T_p is an evidence of the high quality of our sample. Below $T_p = 140$ K, $\varepsilon(T)$ decreases continuously as the temperature is decreased. The peak in $\varepsilon(T)$ is slightly suppressed for the ZFHaFC measurement.

Figures 2(a) and 2(b) show the temperature dependence of $\varepsilon(T)$ cooling in the external magnetic field of 4 T (FC) and upon heating in the same field after field cooling (FHaFC). A deep minimum was observed in the FC state at a temperature ~ 165 K [Fig. 2(a)], while an extremely large peak was obtained in the FHaFC process at the same temperature [Fig. 2(b)]. Using no magnetic field, this peak in $\varepsilon(T)$ during FHaFC shows at $T_p = 140$ K as demonstrated by Fig. 1(b). The applied magnetic field shifts the peak to a higher temperature with a significant rate of $\Delta_H T_p \cong 5$ K per tesla. The value of $\varepsilon(T)$ at the peak increases rapidly with the magnetic field. Therefore, the magnetocapacitance $\Delta\varepsilon/\varepsilon(0) = [\varepsilon(H) - \varepsilon(0)]/\varepsilon(0)$ at the external field $H = 4$ T in the FHaFC state ($\mathbf{H} \parallel c$ -axis) shows very large values as shown in Fig. 3. For

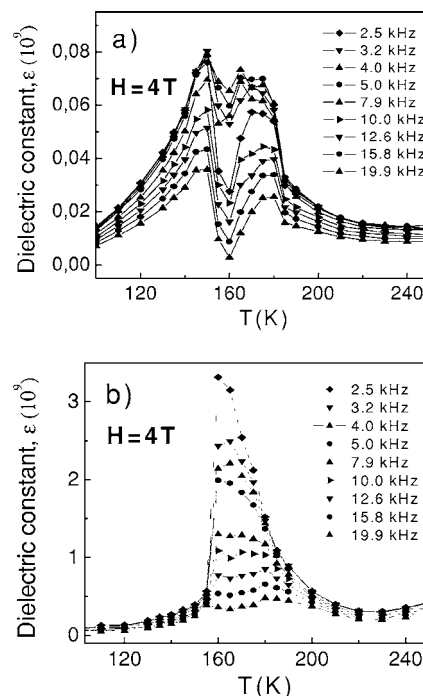


FIG. 2. Temperature dependence of the dielectric permittivity ε in external field of 4 T: (a) FC and (b) FHaFC regimes.

comparison, we show the field dependence of the magnetocapacitance $\Delta\varepsilon/\varepsilon(0)$ for the case where the magnetic field is perpendicular to the c axis at $T = 180$ K in the inset of Fig. 3. It is obvious that colossal magnetocapacitance effect is manifested in the LSM-0.125 single crystal.

The saturation magnetization $M_S(T)$ and magnetic susceptibility $\chi(T)$ are plotted in Fig. 4. Below about 200 K the magnetization varies nonlinearly with the applied field. The value of $M_S(T)$ was determined as the intercept extrapolated to $H = 0$ for the linear portion of the magnetization and $\chi(T)$ as its slope between 1 and 5 T (see the inset in Fig. 4). The sharply increasing magnetization at small magnetic fields is another piece of evidence of the high quality of our sample. A maximum in $\chi(T)$ and the rise of $M_S(T)$ suggest a magnetic transition in the vicinity of 200 K. In addition $\chi(T)$ shows small anomalies at the structural phase transition at 270 K. Similar anomalies at 270 K are also observed in ac magnetic susceptibility.²¹

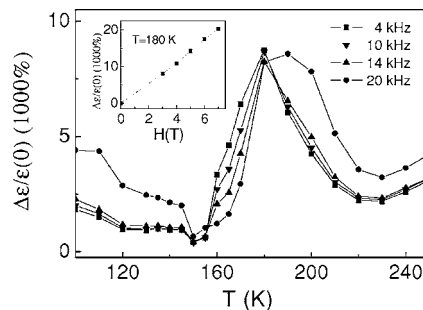


FIG. 3. Temperature dependence of the magnetocapacitance $\Delta\varepsilon/\varepsilon(0) = [\varepsilon(H) - \varepsilon(0)]/\varepsilon(0)$ at $H = 4$ T external field, in the heating regime ($\mathbf{H} \parallel c$ axis); the inset shows field dependence of the magnetocapacitance $\Delta\varepsilon/\varepsilon(0)$ at $T = 180$ K.

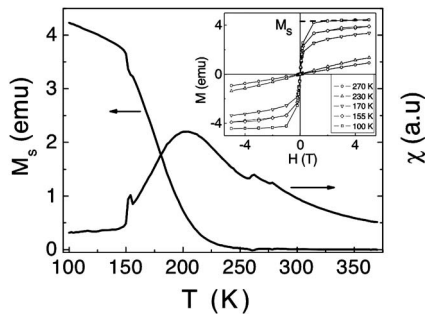


FIG. 4. Temperature dependence of the saturation spontaneous magnetization M_s and of the static magnetic susceptibility χ ($H \parallel c$ axis); the inset shows the field dependence of the magnetization at different temperatures.

Our results on the temperature dependence of the dielectric and magnetic properties show that the LSM-0.125 has large dielectric permittivity and magnetocapacitance at $T < 270$ K. The effects are particularly strong in the temperature range of $140 < T < 185$ K, where the permittivity depends upon the history of applied magnetic field. The strong magnetocapacitance and the field-history-dependent behavior are evidence of the interplay between capacitance and magnetism, as well as spin-glass-like behavior in the temperature range of $140 < T < 185$ K. Below $T = 140$ K an antiferromagnetic long-range orbital order sets in, which makes the in-plane superexchange interaction positive following the Goodenough-Kanamori rule, thus producing a ferromagnetic insulator, in which charges are localized as spin polarons. In the temperature range of $140 < T < 185$ K, the system is magnetic but lacks orbital order. Thus the superexchange interaction can be positive or negative depending on the mutual orientation of the d orbitals on Mn ions, and this is most likely the origin of the spin-glass behavior. We attempted to obtain direct evidence of the spin-glass behavior by magnetic measurements. However, strong ferromagnetic components made the hysteresis in the susceptibility very weak and the results were inconclusive. But some evidence of spin-glass behavior was found at ac and dc magnetic measurements.²¹

According to the pulsed neutron pair-density function (PDF) analysis in LSM- x a doped hole is spread over three Mn sites even when it is localized as a polaron.¹⁴ The insulator-to-metal transition occurs at $x=0.17$ by percolation,^{14,22–26} and the LSM-0.125 we studied is close to the percolation threshold. Thus holes are not totally confined to a single polaron, and there should be a high density of locally connected strings or patches of polarons within which holes can move relative easily. We may characterize this state as the state with nanoscale phase and charge segregation. Since the metallic patches are surrounded by FM or spin-glass insulators, they do not contribute to the dc conductivity, but they do affect the ac conductivity, which leads to a high dielectric constant. Thus the giant dielectric permittivity observed could be called the intrinsic Maxwell-Wagner behavior, because charge dynamics of the metallic areas produce high permittivity.

On the $\text{La}_{1-x}\text{Sr}_x\text{MnO}_3$ phase diagram, increasing Sr concentration results in a metallic state with ferromagnetic order. Therefore, irrespective of the mechanism of phase segrega-

tion (the double-exchange interaction,²⁷ ferrons,²⁸ bipolarons,²⁹ or other models^{3,30}), we can conclude the following: Relatively large patches with multiple holes should be ferromagnetic or superparamagnetic metal. Applied magnetic field will thus promote the formation of such coagulated holes and will influence the distribution of holes in various ways depending on the topology and geometry of the patches. In this line of argument, it is not difficult to see how the applied magnetic field could modify the dielectric response of the system. It is possible that when the system is cooled in a high magnetic field, holes coagulate more intensely to form a higher density of ferromagnetic metal than in the case of the zero-field cooling, which, in turn, increases the dielectric response. This scenario explains the strong magnetocapacitance effect in this system.

Our results suggest that the charge segregation occurs at temperature below 270 K, where the structural transition from a weakly distorted orthorhombic (pseudocubic) phase to the strongly distorted Jahn-Teller orthorhombic phase occurs. An extra increase of the resistivity below 270 K could be explained by the charge segregation. In fact the resistivity is expected to increase when charge segregation occurs without percolation of metallic areas. Thus it reduces the conductivity, as shown in the inset of Fig. 1(b) and increases the dielectric response.

It should be noted that the high values of dielectric permittivity also could arise due to an interfacial polarization and an external Maxwell-Wagner relaxation process.²⁰ Particularly, within this scenario, the CMR effect can lead to a high value of magnetocapacitance coefficient.³¹ Nevertheless, there are several reasons to believe that the giant dielectric permittivity is an intrinsic effect rather than the one caused by the contact areas. (i) The temperature dependence of the ac resistivity of the sample has a weak frequency dependence and the value at low-frequency range agrees with the dc resistivity. (ii) Very different values of the dielectric permittivity are observed at different temperatures even when the value of the conductivity is practically the same (for example, at 135, 160, and 210 K). (iii) Giant dielectric permittivity is observed only at a limited temperature range ($T < 270$ K). (iv) It is also very important that the four-point probe method is used for the measurements.

High values of dielectric response are consistent with the thickness of the insulated areas of $\Delta l \approx 1 \sim 20$ nm ($\Delta l \approx A\epsilon l/\epsilon_0$, where ϵ_0 is the dielectric permittivity in the absence of the charge separation, $\epsilon_0 \approx 60$; A is the unknown coefficient, which takes into account that we have a series of capacitances and the real surface of the metallic region is larger than the sample cross section). This estimate is also consistent with the characteristic dispersion frequency ω_0 ($\omega_0 \sim 10^4 \sim 10^5$ Hz). If we assume the dynamic Maxwell-Wagner effect, the characteristic frequency can be given by $\omega_{MW} = 1/RC$ (in our case $R = 1 \Omega$, $C = 10^{-4} \sim 10^{-5}$ F). Therefore, the low-frequency behavior of the dielectric properties is consistent with the charge dynamics in the nanoregions. But it is impossible to explain such an extreme value of the dielectric permittivity only by the presence of the thin insulated areas, because their number should be large and it suppresses the effect. Therefore, it is necessary to take into account the dynamic character of metallic patches and their

weak interaction with the lattice. Thus, if we take into consideration the motion of the charged metallic patches as a whole in an external electric field, it should help to explain extremely high values of dielectric permittivity. However, further theoretical research is needed before concluding about the effectiveness of such a mechanism.

In conclusion, the temperature dependence of the dielectric and magnetic properties of the $\text{La}_{0.875}\text{Sr}_{0.125}\text{MnO}_3$ single crystals were investigated in a wide range of temperature and external magnetic field. A giant dielectric permittivity was observed at temperatures below 270 K. The features of these properties are attributed to the nanoscale dynamic inhomogeneities appearing at the prepercolation regime of charge ordering. The external magnetic field strongly affects the charge segregation, thus leading to the colossal magnetoca-

pacitance effect. These results can be explained in terms of spin and charge inhomogeneities and their interplay in manganites. While contact effects seem unlikely, the question whether the measured giant dielectric permittivity is caused by either intrinsic Maxwell-Wagner effect or segregated charge dynamics or both of them remains to be clarified.

The authors wish to acknowledge M.I. Balbashov for providing the LSM-0.125 single crystals used in this study. R.F.M. thanks A. M. Bratkovsky and V. V. Kabanov for fruitful discussions. The work at the University of Tennessee was supported by the National Science Foundation through Grant No. DMR04-04781. R.F.M. and S.A.M. are grateful for financial support to the Russian Foundation for Basic Research (Grant No. 05-02-17182).

*Electronic address: mamin@kfti.knc.ru

- ¹S. Jin, T. H. Tiefel, M. McCormack, R. A. Fastnacht, R. Ramesh, and L. H. Chen, *Science* **264**, 413 (1994).
- ²Y. Tokura and N. Nagaosa, *Science* **288**, 462 (2000).
- ³E. Dagotto, T. Hotta, and A. Moreo, *Phys. Rep.* **344**, 1 (2001).
- ⁴A. Urushibura, Y. Moritomo, T. Arima, A. Asamitsu, G. Kido, and Y. Tokura, *Phys. Rev. B* **51**, 14103 (1995).
- ⁵Y. Moritomo, A. Asamitsu, and Y. Tokura, *Phys. Rev. B* **56**, 12190 (1997).
- ⁶V. Yu. Ivanov, V. D. Travkin, A. A. Mukhin, S. P. Lebedev, A. A. Volkov, A. Pimenov, A. Loidl, A. M. Balbashov, and A. V. Mozhaev, *J. Appl. Phys.* **83**, 7180 (1998); M. Paraskevopoulos, F. Mayr, C. Hartinger, A. Pimenov, J. Hemberger, P. Lunkenheimer, A. Loidl, A. A. Mukhin, V. Yu. Ivanov, and A. M. Balbashov, *J. Magn. Magn. Mater.* **211**, 118 (2000).
- ⁷H. Kawano, R. Kajimoto, M. Kubota, and H. Yoshizawa, *Phys. Rev. B* **53**, R14709 (1996).
- ⁸Y. Yamada, O. Hino, S. Nohdo, R. Kanao, T. Inami, and S. Katano, *Phys. Rev. Lett.* **77**, 904 (1996).
- ⁹Y. Endoh, K. Hirota, S. Ishihara, S. Okamoto, Y. Murakami, A. Nishizawa, T. Fukuda, H. Kimura, H. Nojiri, K. Kaneko, and S. Maekawa, *Phys. Rev. Lett.* **82**, 4328 (1999).
- ¹⁰F. Mayr, C. Hartinger, M. Paraskevopoulos, A. Pimenov, J. Hemberger, A. Loidl, A. A. Mukhin, and A. M. Balbashov, *Phys. Rev. B* **62**, 15673 (2000).
- ¹¹T. Kimura *et al.*, *Nature (London)* **426**, 55 (2003); T. Goto, T. Kimura, G. Lawes, A. P. Ramirez, and Y. Tokura, *ibid.* **92**, 257201 (2004).
- ¹²S. Weber, P. Lunkenheimer, R. Fichtl, J. Hemberger, V. Tsurkan, and A. Loidl, *Phys. Rev. Lett.* **96**, 157202 (2006).
- ¹³A. L. Efros and B. I. Shklovskii, *Phys. Status Solidi B* **76**, 475 (1976).
- ¹⁴D. Louca, T. Egami, E. L. Brosha, H. Röder, and A. R. Bishop, *Phys. Rev. B* **56**, R8475 (1997).
- ¹⁵R. V. Demin, L. I. Koroleva, and A. M. Balbashov, *JETP Lett.* **70**, 314 (1999).
- ¹⁶J. Deisenhofer, D. Braak, H.-A. Krug von Nidda, J. Hemberger, R. M. Eremina, V. A. Ivashin, A. M. Balbashov, G. Jug, A. Loidl, T. Kimura, and Y. Tokura, *Phys. Rev. Lett.* **95**, 257202 (2005).
- ¹⁷N. Biskup, A. de Andres, J. L. Martinez, and C. Perca, *Phys. Rev. B* **72**, 024115 (2005).
- ¹⁸M. P. Gutiérrez, J. Mira, and J. Rivas, *Phys. Lett. A* **323**, 473 (2004).
- ¹⁹J. L. Cohn, M. Peterca, and J. J. Neumeier, *J. Appl. Phys.* **97**, 034102 (2005).
- ²⁰P. Lunkenheimer, V. Bobnar, A. V. Pronin, A. I. Ritus, A. A. Volkov, and A. Loidl, *Phys. Rev. B* **66**, 052105 (2002). P. Lunkenheimer, R. Fichtl, S. G. Ebbinghaus, and A. Loidl, *ibid.* **70**, 172102 (2004).
- ²¹J. Nogues, V. Skumryev, J. S. Munoz, B. Martinez, J. Fontcuberta, L. Pinsard, and A. Revcolevschi, *Phys. Rev. B* **64**, 024434 (2001); B. Martinez, V. Laukhin, J. Fontcuberta, J. Nogues, V. Skumryev, J. S. Munoz, L. Pinsard, and A. Revcolevschi, *J. Appl. Phys.* **89**, 6633 (2001).
- ²²S. Yunoki, J. Hu, A. L. Malvezzi, A. Moreo, N. Furukawa, and E. Dagotto, *Phys. Rev. Lett.* **80**, 845 (1998).
- ²³S. Yunoki, A. Moreo, and E. Dagotto, *Phys. Rev. Lett.* **81**, 5612 (1998).
- ²⁴M. Mayr, A. Moreo, J. A. Vergés, J. Arispe, A. Feiguin, and E. Dagotto, *Phys. Rev. Lett.* **86**, 135 (2001).
- ²⁵T. Egami, in *Structure and Bonding* edited by J. B. Goodenough (Springer-Verlag, Berlin, 2001), Vol. 98, p. 115.
- ²⁶M. Yu. Kagan and K. I. Kugel, *Phys. Usp.* **44**, 553 (2001).
- ²⁷C. Zener, *Phys. Rev. B* **82**, 403 (1951).
- ²⁸E. L. Nagaev, *Phys. Rev. B* **60**, R6984 (1999).
- ²⁹A. S. Alexandrov, A. M. Bratkovsky, and V. V. Kabanov, *Phys. Rev. Lett.* **96**, 117003 (2006).
- ³⁰A. J. Millis, P. B. Littlewood, and B. I. Shraiman, *Phys. Rev. Lett.* **74**, 5144 (1995).
- ³¹G. Catalan, *Appl. Phys. Lett.* **88**, 102902 (2006).